NUCLEAR SCIENCE AND ENGINEERING: **166**, 239–253 (2010)

A Discrete Generalized Multigroup Energy Expansion Theory

Lei Zhu and Benoit Forget*

Massachusetts Institute of Technology, Department of Nuclear Science and Engineering
77 Massachusetts Avenue, Cambridge, Massachusetts

Received October 27, 2009
Accepted May 25, 2010

Abstract—*This study describes the generalized multigroup energy treatment for the neutron transport equation. Discrete Legendre orthogonal polynomials (DLOPs) are used to expand the energy dependence of the angular flux into a set of flux moments. The leading (zeroth)–order equation is identical to a standard multigroup solution, while the higher-order equations are decoupled from each other and only depend on the leading-order solution because of the orthogonality property of the DLOPs. This decoupling leads to computational times comparable to the coarse-group calculation but provides an accurate fine-group energy spectrum. One-dimensional single-assembly and core calculations were performed to demonstrate the potential of the discrete generalized multigroup method. Computational results show that the discrete generalized multigroup method can produce an accurate fine-group whole-core solution for less computational time. A source update process is also introduced that provides improvement of integral quantities such as eigenvalue and reaction rates over the coarse-group solution.*

I. INTRODUCTION

The goal of this paper is to develop a generalized multigroup energy treatment for the neutron transport equation that will reduce the computational cost needed for high-fidelity modeling of nuclear reactors. Current core-level deterministic methods rely entirely on the multigroup energy treatment of the nuclear cross sections. In the energy condensation process, reaction rates are conserved based on the knowledge of the exact energy spectrum. Since this quantity is unknown a priori, a multilevel approach is used to refine the flux spectrum approximation, which is then used to condense the cross sections into a smaller number of groups. The finer group structure is thus condensed to a more manageable coarse cross-section set in terms of computational resources and number of coupled equations to solve. As the number of energy groups is reduced, spatial detail is added going from a one-dimensional (1-D) pin cell to a two-dimensional (2-D) fuel assembly to an eventual full three-dimensional (3-D) core. This process is obviously cumbersome and also leads to a considerable loss of energy resolution. While such an approach has proven sufficient for current reactors for which many experiments were performed, it is envisioned that high-fidelity core modeling will require thousands of energy groups if one desires to improve the predictive capability of the simulation. Increasing the number of energy groups allows for a better representation of the resonance region and a more accurate spectral description but comes with a substantial computational cost as the number of energy groups directly relates to the number of equations to be solved simultaneously.

In this study, a fundamentally new discrete generalized multigroup (DGM) method is developed that can recover the fine-group energy spectrum with a computational cost comparable to the standard coarse-group calculation. In the DGM method, the fine-group assembly solution is used as the weighting function for the generation of the coarse-group cross sections and associated moments. These cross-section moments are then inserted in the transport equation to provide a flux solution with associated moments. The obtained flux moments can be unfolded to construct a whole-core energy spectrum that is an accurate estimate of the fine-group solution. The higher-order moments of the flux are decoupled from each other and only depend on the zeroth-order solution because of the orthogonality property of the discrete Legendre orthogonal polynomials (DLOPs). This decoupling results in a computational cost comparable to the coarse-group calculation while

*E-mail: bforget@mit.edu

still producing an energy spectrum comparable to the fine-group solution.

The leading-order solution is equivalent to the standard coarse-group solution, and thus, integral quantities, i.e., the eigenvalue and reaction rates, are identical to those obtained from the coarse-group calculation. However, a further step can be used to update the eigenvalue and flux, thus improving these integral quantities vis-à-vis the fine-group calculation with very little added computational cost. Thus, the newly developed DGM method is capable of improving both the energy spectrum and the integral quantities.

Section II describes relevant work in the field of energy discretization, while Sec. III presents the derivation of the DGM method. Section IV presents results of the 1-D implementation of the method with concluding remarks and future work following in Sec. V.

II. BACKGROUND

The standard multigroup method is the most universally applied method to discretize the energy dependence in neutron transport theory and can be very accurate if a large number of energy groups are used.[1] Condensation to a more manageable data set requires a priori knowledge of the flux spectrum, commonly approximated by pin-cell and/or lattice calculations. While the multigroup method is the workhorse of the current reactor simulations, the piecewise constant solution within each energy group greatly diminishes the energy resolution within each energy interval.

An alternate approach that was proposed is the use of pointwise data in deterministic transport calculations. Williams, Asgari, and Hollenbach developed the 1-D discrete ordinates code CENTRM, which treats part of the nuclear data as pointwise cross sections.[2] The method uses a combination of multigroup and pointwise cross sections to obtain a very accurate neutron spectrum. The "submoment" expansion technique is used to accurately evaluate the scattering transfer function. CENTRM is currently used in the SCALE package to generate resonance shielded multigroup data. The code solves a fixed-source transport equation in infinite media or 1-D pin-type geometries.

The RAZOR lattice code developed by Zerkle et al. also proposes using a near-continuous energy pointwise solution method to the transport equation.[3] This method was developed to improve the resonance energy treatment within the multigroup methodology and uses pointwise data to generate the multigroup data.

Attieh and Pevey developed a generalized multigroup method by introducing "chapeau" functions.[4] The new method allows energy to have partial membership in more than one group and thus allows the assumed group spectral shape to adapt to problem-dependent conditions. The method was tested in an infinite homogeneous problem with different numbers of energy groups.

The opacity distribution function (ODF) concept was initially introduced by Chandrasekar in 1935 to represent a range of opacities within a frequency interval that he used to study stellar radiation, and it was subsequently used in model-atmosphere calculations by Strom and Kurucz in 1966 (Ref. 5). The ODF method separates the frequency domain into intervals somewhat equivalent to the multigroup concept in reactor physics. The opacity in each interval is then distributed as a probability distribution function (pdf) over the opacity range covered. The pdf is most often represented by a histogram. This methodology allows for frequency variations within the interval when performing the calculations, but all the frequency dependence within an interval is lost. The approach is conceptually very similar to the proposed DGM method; however, the DGM method has the added advantage of conserving the energy dependence within each group.

In previous papers, a generalized multigroup method was developed.[6,7] This was achieved by generalizing the standard condensation procedure, assuming that the energy dependence of the neutron flux (spectrum) could be expanded in a set of orthogonal basis functions, and folding this dependence into the cross-section condensation process. It was shown that the standard condensation procedure is contained within this generalized method as a zeroth-order approximation and that through implementing this method, the computational time is reduced to that of standard coarse-group computations but with the detail usually associated with much finer group solutions. The validity of the method was demonstrated with a 1-D S_N transport code with a Legendre polynomial expansion of the energy variable on 1-D problems of varying heterogeneity. The results showed that a few-group solution could provide a continuous-energy flux spectrum that closely matched a much finer group solution. The proposed DGM method in this study is very similar in nature but has proven more appropriate for the commonly discrete energy treatment in deterministic codes. Instead of using a continuous orthogonal expansion, this study proposes the use of a discrete orthogonal expansion. The discrete expansion is a more appropriate fit in the multigroup framework and provides enormous advantages over the previous formulation as will be shown in this paper. A detailed comparison of the discrete and continuous expansion methods is given in Sec. III.C.

III. METHOD

This section gives a brief overview, for sake of completeness, of the DLOPs and their properties. This is followed by the derivation of the DGM method in which the DLOPs are used. Similar derivations can be

made with other discrete orthogonal expansion without much loss of generality. Following the derivation is a detailed comparison between the DGM method and the continuous-energy expansion method.

III.A. Discrete Legendre Orthogonal Polynomials

The DLOPs were introduced by Neuman and Schonbach in 1974 and are a set of orthogonal polynomials of a discrete independent variable that are assumed to be only a finite number of values in the interval.[8] Mathematically, the DLOPs $P_m(K,N)$ are defined over the discrete interval $K = 0,1,2,\ldots,N$, and $m = 0,1,2,\ldots,N$ is the degree of the polynomial. Their orthogonality relation can be expressed as

$$\sum_{K=0}^{N} P_m(K,N)P_l(K,N) = \frac{\delta_{ml}}{a_m} \ , \tag{1}$$

where δ_{ml} is the Kronecker Delta and the normalization constant a_m is

$$a_m = (2m+1)\frac{N^{(m)}}{(N+m+1)^{(m+1)}} \ , \tag{2}$$

where $N^{(m)}$ is the m'th fading factorial of N defined as

$$N^{(m)} = \begin{cases} N(N-1)(N-2)\ldots(N-m+1) \ , & m > 0 \\ 1 \ , & m = 0 \end{cases} . \tag{3}$$

The normalization relation is

$$P_m(0,N) = 1 \quad \text{for all } m \ . \tag{4}$$

An explicit expression of $P_m(K,N)$ is

$$\begin{aligned} P_m(K,N) &= \sum_{j=0}^{m} (-1)^j \binom{m}{j}\binom{m+j}{j}\frac{K^{(j)}}{N^{(j)}} \\ &= \sum_{j=0}^{m} l(m,j)\frac{K^{(j)}}{N^{(j)}} \end{aligned} \tag{5}$$

for $m = 0,1,2,\ldots,N$. The coefficients $l(m,j)$ are identical to those of the shifted Legendre polynomials on the interval [0,1] apart from the sign.

One of the most important properties of the DLOPs to be used in the DGM method derivation comes from the othogonality relation in Eq. (1) by setting $m = 0$ to obtain

$$\sum_{K=0}^{N} P_l(K,N) = \frac{\delta_{0l}}{a_0} \ , \tag{6}$$

in which the following fact is used:

$$P_0(K,N) = 1 \quad \text{for all } K \ . \tag{7}$$

III.B. Method Derivation

Our starting point for the derivation is the time-independent integrodifferential neutron transport equation with no external sources (i.e., eigenvalue problem). A similar procedure can be applied readily to a source-driven problem, time-dependent problems, or other forms of the transport equation:

$$\begin{aligned} &\vec{\Omega}\cdot\nabla\psi(\vec{r},\vec{\Omega},E) + \sigma_t(\vec{r},E)\psi(\vec{r},\vec{\Omega},E) \\ &\quad = \int_0^\infty dE' \int_{4\pi} d\vec{\Omega}'\, \sigma_s(\vec{r},\vec{\Omega}'\to\vec{\Omega},E'\to E) \\ &\qquad \times \psi(\vec{r},\vec{\Omega}',E') + \frac{\chi(\vec{r},E)}{4\pi k}\int_0^\infty dE' \\ &\qquad \times \int_{4\pi} d\vec{\Omega}'\, \nu\sigma_f(\vec{r},E')\psi(\vec{r},\vec{\Omega}',E') \ , \end{aligned} \tag{8}$$

where the angular neutron flux is represented by ψ with phase space variables: r for all three spatial components, Ω for the solid angle, and E for the energy. The total and fission macroscopic cross sections are represented by σ_t and σ_f, respectively. The fission energy spectrum is represented by χ, and the scattering transfer function is denoted by σ_s. If the energy spectrum is separated into G coarse groups, the scattering kernel can be expressed using spherical harmonics, and assuming fission to be isotropic, Eq. (8) in coarse group g with energy E_g can be written as

$$\begin{aligned} &\vec{\Omega}\cdot\nabla\psi(\vec{r},\vec{\Omega},E_g) + \sigma_t(\vec{r},E_g)\psi(\vec{r},\vec{\Omega},E_g) \\ &\quad = \sum_{g'=1}^{G}\sum_{l=0}^{\infty}\sum_{m=-l}^{l} \frac{Y_{lm}^*(\vec{\Omega})}{4\pi}\int_{\Delta E_{g'}} dE_{g'}\, \sigma_{sl}(\vec{r},E_{g'}\to E_g) \\ &\qquad \times \phi_{lm}(\vec{r},E_{g'}) + \frac{\chi(\vec{r},E_g)}{4\pi k} \\ &\qquad \times \sum_{g'=1}^{G}\int_{\Delta E_{g'}} dE_{g'}\, \nu\sigma_f(\vec{r},E_{g'})\phi(\vec{r},E_{g'}) \ . \end{aligned} \tag{9}$$

Equation (9) thus separates the transport equation over G coarse groups, but the energy is still continuous within each group. It is now possible to apply the multigroup methodology within each coarse group g as

$$\begin{aligned} &\vec{\Omega}\cdot\nabla\psi(\vec{r},\vec{\Omega},K) + \sigma_t(\vec{r},K)\psi(\vec{r},\vec{\Omega},K) \\ &\quad = \sum_{g'=1}^{G}\sum_{l=0}^{\infty}\sum_{m=-l}^{l} \frac{Y_{lm}^*(\vec{\Omega})}{4\pi}\sum_{L=0}^{M-1}\sigma_{sl}(\vec{r},L\to K)\phi_{lm}(\vec{r},L) \\ &\qquad + \frac{\chi(\vec{r},K)}{4\pi k}\sum_{g'=1}^{G}\sum_{L=0}^{M-1}\nu\sigma_f(\vec{r},L)\phi(\vec{r},L) \ . \end{aligned} \tag{10}$$

In going from Eq. (9) to Eq. (10), it is assumed that there are N fine-group points within coarse group g with point index $K = 0,1,2,\ldots,N-1$, and M fine-group points within coarse group g' with point index $L = 0,1,2,\ldots,M-1$. This is equivalent to having an ultrafine multigroup equation where each coarse group has varying fine-group structure.

The following step is to expand the energy dependence of the angular flux into a set of DLOP moments (any other discrete orthogonal set would also work). The energy dependence of the angular flux in Eq. (10) can be expanded using DLOPs within each coarse group g as

$$\psi(\vec{r},\vec{\Omega},K) = \sum_{i=0}^{N-1} a_i P_i(K,N-1)\psi_{ig}(\vec{r},\vec{\Omega}) \ , \qquad (11)$$

where

$\Delta E_K \in \Delta E_g$

$K = 0,\ldots,N-1 =$ index of the fine energy group point within the coarse group g

$N =$ total number of fine-group points within the coarse group g,

and a_i is defined in Eq. (2). The flux moments can be obtained from the orthogonality relation:

$$\psi_{ig}(\vec{r},\vec{\Omega}) = \sum_{K=0}^{N-1} P_i(K,N-1)\psi(\vec{r},\vec{\Omega},K) \ . \qquad (12)$$

Substituting Eq. (11) into Eq. (10), and then multiplying and summing by $\sum_{K=0}^{N-1} P_i(K,N-1)$ to obtain

$$\begin{aligned}\vec{\Omega}\cdot\nabla\psi_{ig}(\vec{r},\vec{\Omega}) &+ \sigma_{t,ig}(\vec{r},\vec{\Omega})\psi_{ig}(\vec{r},\vec{\Omega}) \\ &= \sum_{K=0}^{N-1} P_i(K,N-1) \sum_{g'=1}^{G}\sum_{l=0}^{\infty}\sum_{m=-l}^{l} \frac{Y_{lm}^*(\vec{\Omega})}{4\pi} \\ &\quad\times \sum_{L=0}^{M-1} \sigma_{sl}(\vec{r},L\to K)\phi_{lm}(\vec{r},L) \\ &\quad + \frac{\chi_{ig}(\vec{r})}{4\pi k}\sum_{g'=1}^{G}\sum_{L=0}^{M-1}\nu\sigma_f(\vec{r},L)\phi(\vec{r},L) \ , \end{aligned} \qquad (13)$$

where $\psi_{ig}(\vec{r},\vec{\Omega})$ is defined in Eq. (12) and where

$$\chi_{ig}(\vec{r}) = \sum_{K=0}^{N-1} P_i(K,N-1)\chi(\vec{r},K) \qquad (14)$$

and

$$\sigma_{t,ig}(\vec{r},\vec{\Omega}) = \frac{\sum_{K=0}^{N-1} P_i(K,N-1)\sigma_t(\vec{r},K)\psi(\vec{r},\vec{\Omega},K)}{\sum_{K=0}^{N-1} P_i(K,N-1)\psi(\vec{r},\vec{\Omega},K)} \ . \qquad (15)$$

A multigroup equation is now obtained in which each coarse group g contains an expanded flux. The zeroth order of this expansion reverts directly to the well-known multigroup approximation, and all higher orders offer information of the spectrum within each coarse group. Additionally, as was done in Ref. 7, we define the total cross section as the mean within the coarse group g and a higher-order perturbation term:

$$\sigma_t(\vec{r},K) = \sigma_{t,0g}(\vec{r}) + \delta_g(\vec{r},K) \ , \qquad (16)$$

where

$$\sigma_{t,0g}(\vec{r}) = \frac{\sum_{K=0}^{N-1}\sigma_t(\vec{r},K)\phi(\vec{r},K)}{\sum_{K=0}^{N-1}\phi(\vec{r},K)} \ , \qquad (17)$$

and thus define

$$\delta_{ig}(\vec{r},\vec{\Omega}) = \frac{\sum_{K=0}^{N-1} P_i(K,N-1)\delta_g(\vec{r},K)\psi(\vec{r},\vec{\Omega},K)}{\sum_{K=0}^{N-1} P_0(K,N-1)\psi(\vec{r},\vec{\Omega},K)} \ . \qquad (18)$$

The advantage of this δ-term approximation is that only the zeroth-order flux appears in the denominators, which makes the method more stable numerically in the presence of cross-section moments that are near zero. Equation (13) thus becomes

$$\begin{aligned}\vec{\Omega}\cdot\nabla\psi_{ig}(\vec{r},\vec{\Omega}) &+ \sigma_{t,0g}(\vec{r})\psi_{ig}(\vec{r},\vec{\Omega}) + \delta_{ig}(\vec{r},\vec{\Omega})\psi_{0g}(\vec{r},\vec{\Omega}) \\ &= \sum_{K=0}^{N-1} P_i(K,N-1) \sum_{g'=1}^{G}\sum_{l=0}^{\infty}\sum_{m=-l}^{l} \frac{Y_{lm}^*(\vec{\Omega})}{4\pi} \\ &\quad\times \sum_{L=0}^{M-1} \sigma_{sl}(\vec{r},L\to K)\phi_{lm}(\vec{r},L) \\ &\quad + \frac{\chi_{ig}(\vec{r})}{4\pi k}\sum_{g'=1}^{G}\sum_{L=0}^{M-1}\nu\sigma_f(\vec{r},L)\phi(\vec{r},L) \ . \end{aligned} \qquad (19)$$

The next step is to treat the scattering and fission terms on the right hand side (RHS) by preserving the reaction rates. The reaction rates can be defined as

$$R_f(\vec{r},L) = \nu\sigma_f(\vec{r},L)\phi(\vec{r},L) \qquad (20)$$

and

$$R_{s,lm}(\vec{r},L\to K) = \sigma_{sl}(\vec{r},L\to K)\phi_{lm}(\vec{r},L) \ . \qquad (21)$$

Expanding both the reaction rates in the following way:

$$R(\vec{r},L) = \sum_{j=0}^{M-1} a_j P_j(L,M-1)R_{jg}(\vec{r}) \ , \qquad (22)$$

where

$$R_{jg}(\vec{r}) = \sum_{L=0}^{M-1} P_j(L, M \to 1) R(\vec{r}, L) \ . \tag{23}$$

By the treatment of orthogonal expansion in Eq. (22), the reaction rates are preserved. The *RHS* of Eq. (19) becomes

$$\begin{aligned} RHS = & \sum_{K=0}^{N-1} P_i(K, N-1) \sum_{g'=1}^{G} \sum_{l=0}^{\infty} \sum_{m=-l}^{l} \frac{Y_{lm}^*(\vec{\Omega})}{4\pi} \sum_{L=0}^{M-1} \sum_{j=0}^{M-1} a_j P_j(L, M-1) R_{s,lm,jg'}(\vec{r}, K) \\ & + \frac{\chi_{ig}(\vec{r})}{4\pi k} \sum_{g'=1}^{G} \sum_{L=0}^{M-1} \sum_{j=0}^{M-1} a_j P_j(L, M-1) R_{f,jg'}(\vec{r}) \\ = & \sum_{g'=1}^{G} \sum_{l=0}^{\infty} \sum_{m=-l}^{l} \sum_{j=0}^{M-1} \frac{Y_{lm}^*(\vec{\Omega})}{4\pi} \sum_{K=0}^{N-1} P_i(K, N-1) a_j R_{s,lm,jg'}(\vec{r}, K) \sum_{L=0}^{M-1} P_j(L, M-1) \\ & + \frac{\chi_{ig}(\vec{r})}{4\pi k} \sum_{g'=1}^{G} \sum_{j=0}^{M-1} a_j R_{f,jg'}(\vec{r}) \sum_{L=0}^{M-1} P_j(L, M-1) \ . \end{aligned} \tag{24}$$

Now applying the property of DLOPs stated in Eq. (6), only the zeroth-order terms ($j = 0$) remain on the *RHS*. The *RHS* can thus be simplified as

$$\begin{aligned} RHS = & \sum_{g'=1}^{G} \sum_{l=0}^{\infty} \sum_{m=-l}^{l} \frac{Y_{lm}^*(\vec{\Omega})}{4\pi} \sum_{K=0}^{N-1} P_i(K, N-1) R_{s,lm,0g'}(\vec{r}, K) + \frac{\chi_{ig}(\vec{r})}{4\pi k} \sum_{g'=1}^{G} R_{f,0g'}(\vec{r}) \\ = & \sum_{g'=1}^{G} \sum_{l=0}^{\infty} \sum_{m=-l}^{l} \frac{Y_{lm}^*(\vec{\Omega})}{4\pi} \sum_{K=0}^{N-1} P_i(K, N-1) \sum_{L=0}^{M-1} \sigma_{sl}(\vec{r}, L \to K) \phi_{lm}(\vec{r}, L) + \frac{\chi_{ig}(\vec{r})}{4\pi k} \sum_{g'=1}^{G} \sum_{L=0}^{M-1} \nu\sigma_f(\vec{r}, L) \phi(\vec{r}, L) \\ = & \sum_{g'=1}^{G} \sum_{l=0}^{\infty} \sum_{m=-l}^{l} \frac{Y_{lm}^*(\vec{\Omega})}{4\pi} \sigma_{s,lm,i,g' \to g}(\vec{r}) \phi_{lm,g'}(\vec{r}) + \frac{\chi_{ig}(\vec{r})}{4\pi k} \sum_{g'=1}^{G} \nu\sigma_{f,g'}(\vec{r}) \phi_{g'}(\vec{r}) \ , \end{aligned} \tag{25}$$

where the coarse-group scalar flux and the coarse-group fission and scattering cross sections are given by

$$\phi_{g'}(\vec{r}) = \sum_{L=0}^{M-1} \phi(\vec{r}, L) \ , \tag{26}$$

$$\phi_{lm,g'}(\vec{r}) = \sum_{L=0}^{M-1} \phi_{lm}(\vec{r}, L) \ , \tag{27}$$

$$\nu\sigma_{f,g'}(\vec{r}) = \frac{\sum_{L=0}^{M-1} \nu\sigma_f(\vec{r}, L) \phi(\vec{r}, L)}{\sum_{L=0}^{M-1} \phi(\vec{r}, L)} \ , \tag{28}$$

and

$$\sigma_{s,lm,i,g' \to g}(\vec{r}) = \frac{\sum_{L=0}^{M-1} \phi_{lm}(\vec{r}, L) \sum_{K=0}^{N-1} P_i(K, N-1) \sigma_{sl}(\vec{r}, L \to K)}{\sum_{L=0}^{M-1} \phi_{lm}(\vec{r}, L)} \ . \tag{29}$$

Finally, the transport equation with DLOP expansion becomes

$$\vec{\Omega}\cdot\nabla\psi_{ig}(\vec{r},\vec{\Omega}) + \sigma_{t,0g}(\vec{r})\psi_{ig}(\vec{r},\vec{\Omega}) + \delta_{ig}(\vec{r},\vec{\Omega})\psi_{0g}(\vec{r},\vec{\Omega})$$
$$= \sum_{g'=1}^{G}\sum_{l=0}^{\infty}\sum_{m=-l}^{l}\frac{Y_{lm}^{*}(\vec{\Omega})}{4\pi}\sigma_{s,lm,i,g'\to g}(\vec{r})\phi_{lm,g'}(\vec{r})$$
$$+ \frac{\chi_{ig}(\vec{r})}{4\pi k}\sum_{g'=1}^{G}\nu\sigma_{f,g'}(\vec{r})\phi_{g'}(\vec{r}) \quad . \tag{30}$$

The zeroth-order ($i = 0$) calculation is equivalent to the standard coarse-group calculation, and Eqs. (26) through (29) can be determined by the zeroth-order calculation. From Eq. (25) it can be seen that the higher-order equations are decoupled from each other and only depend on the zeroth-order (coarse-group) flux. This decoupling leads to computational costs comparable to the common multigroup solution over G coarse groups (higher-order equations are solved very quickly since their *RHS* is known) but can give a fine-group energy spectrum by the unfolding of the angular flux from all the moments:

$$\psi(\vec{r},\vec{\Omega},K) = \sum_{i=0}^{N-1} a_i P_i(K,N-1)\psi_{ig}(\vec{r},\vec{\Omega}) \quad . \tag{31}$$

III.C. More Discussion on the Discrete and Continuous-Energy Expansions

The continuous form of the generalized multigroup theory proved very promising, but the presence of negative fluxes limited its application. While ongoing work is focusing on fixing these shortcomings, the idea of using discrete orthogonal polynomials was studied. For example, let us assume a master library composed of 4 energy groups in the 1×10^{-10}-MeV to 20-MeV range. In the continuous-energy derivation of a fine-group database from a multigroup library, the energy boundaries of the energy groups are needed, and a cross-section moment database can be built. Since this database is essentially trying to represent step functions over ten orders of magnitude in energy (i.e., trying to represent the fine-group data), a very large–order polynomial is needed for an accurate representation. Additionally, high-order polynomials will also lead to oscillations that may have negative values as illustrated in Fig. 1 in which an example step function with $n = 4$ piecewise constant value is approximated with 20- and 100-order expansions, respectively.

The previous continuous derivation in Refs. 6 and 7 is thus much more appropriate for representing continuous-energy data, but this adds quite a bit of complexity to its application with deterministic codes. In the discrete derivation, the master library of four groups is considered as discrete points with integer values of 1 to 4; thus, there is no need for the energy boundaries of the groups. The cross-section moments are limited to a third-order expansion but reproduce the information contained in the four-group library exactly. When discretizing the energy variable, the discrete expansion methodology is thus much more accurate and requires fewer moments. For example, approximating the step function of Fig. 1 by applying a third $(n - 1)$ order discrete expansion recovers exactly the height of the four step values (y), as shown in Fig. 2. Note that the expansion order is fixed at $n - 1$ because of the definition of DLOPs. Furthermore, one only needs to know the number of discretization domains$(n = 4)$, while the

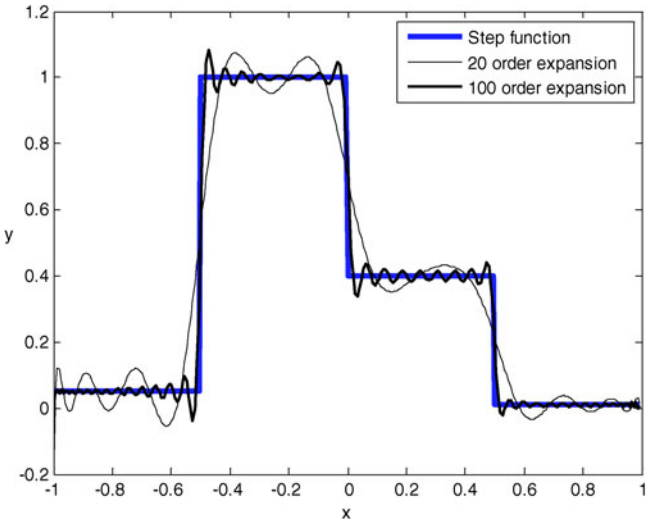

Fig. 1. Expansion of a step function using continuous Legendre polynomials.

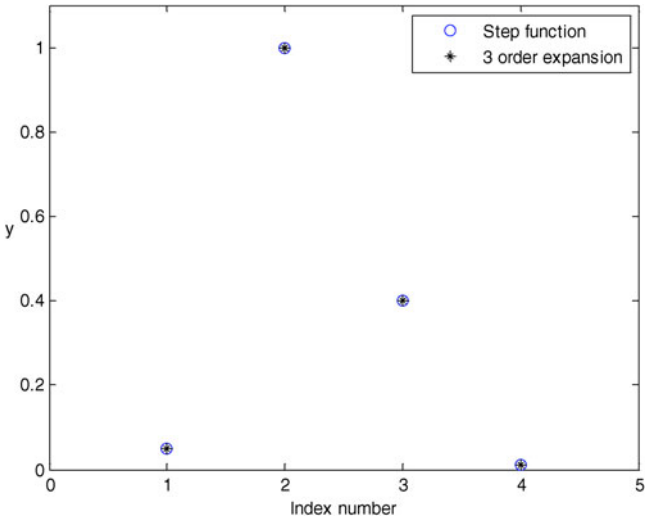

Fig. 2. Expansion of a step function using discrete Legendre polynomials.

information of where the domains start and end is not required, i.e., $x \in (-1.0, -0.5)$, $(-0.5, 0.0)$, $(0.0, 0.5)$, and $(0.5, 1.0)$, respectively, in this example.

For the sake of clarity, another example is in order. Assuming a fine-group library of 100 groups, a coarse-group library of four energy groups can be formed (e.g., 25 groups in each) that is condensed from an estimated energy spectrum. The system of four equations (assuming only energy) would correspond to the multigroup method, but the DGM method also provides 24 other equations for each of the four zeroth-order equations that provide additional information about the energy spectrum. These additional equations are all independent of each other and only depend on the initial zeroth-order solution.

IV. COMPUTATIONAL RESULTS

In 1-D discrete ordinates, assuming isotropic scattering and applying transport cross sections as a linear anisotropic scattering approximation, Eq. (30) can be written as

$$\mu \frac{\partial \psi_{ig}(x,\mu)}{\partial x} + \sigma_{tr,0g}(x)\psi_{ig}(x,\mu) + \delta_{ig}(x,\mu)\psi_{0g}(x,\mu)$$

$$= \frac{1}{2}\sum_{g'=1}^{G} \sigma_{s,i,g'\to g}(x)\phi_{g'}(x)$$

$$+ \frac{\chi_{ig}(x)}{2k}\sum_{g'=1}^{G} \nu\sigma_{f,g'}(x)\phi_{g'}(x) \quad , \tag{32}$$

where the transport cross-section moments and the perturbation term are defined in the same way as Eqs. (15) through (18) by using transport cross-section data instead of total cross-section data.

A 1-D discrete ordinates code was written to test out the DGM method on several 1-D reactor problems typical of boiling water reactor (BWR) core configurations, each composed of seven fuel assemblies. The full description of these problems, illustrated in Fig. 3, can be found in Ref. 7. The method was tested on all four assemblies and three cores. The current implementation is limited to 1-D discrete ordinates, but the extension to other solution techniques of the transport equation or diffusion equation is straightforward. It should also be noted that the 1-D discrete ordinates implementation includes no form of acceleration as this facilitates the comparison between methods. However, it should be noted that acceleration techniques would most certainly reduce the computational time disparity presented in these results.

IV.A. Single-Assembly Tests

The DGM method was initially tested on each of the four assemblies. It should also be noted that for this first test case, the cross-section moments were generated with the exact reference spectrum; thus, the goal of this test is to verify the accuracy of the approximation made in the DGM method. In this implementation, an eight-group cross-section database serves as our fine-group structure and is used to calculate our reference solution. The DGM method is applied to a one-group database with seventh-order expansion condensed from the reference solution. Both the reference and the DGM calculations are performed using an S_{16} angular approximation and the same

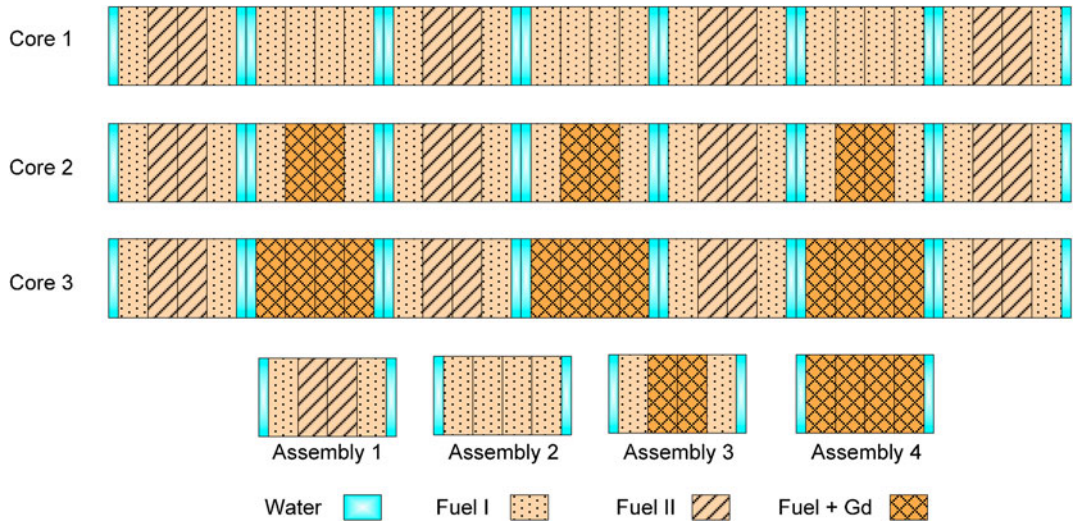

Fig. 3. Core and assembly configurations.

spatial mesh. The flux is converged to 10^{-5}, and the eigenvalue is converged to within 10^{-6}. Reflective boundary conditions are set on both sides. The step difference method is applied in the spatial sweep process.

If the assembly has I spatial points and the reference and DGM solutions have H fine groups and G coarse groups with expansion, respectively, the relative error RE with the fine energy group and spatial mesh point indices h and i are defined as

$$RE(i,h) = \left| \frac{\phi_H(i,h) - \phi_{G/\exp}(i,h)}{\phi_H(i,h)} \right| , \quad (33)$$

where

$\phi_H(i,h)$ = group scalar flux from the fine-group calculation

$\phi_{G/\exp}(i,h)$ = unfolded group scalar flux from the G coarse group with expansion calculation.

In terms of this pointwise relative error, the average relative error err_{avg}, mean relative error err_{mean}, root mean square relative error err_{rms}, and maximum relative error $err_{\max}$ of the scalar flux are defined as

$$err_{avg} = \frac{1}{I \times H} \sum_{i=1}^{I} \sum_{h=1}^{H} RE(i,h) , \quad (34)$$

and

$$err_{mean} = \frac{1}{I \times H} \sum_{i=1}^{I} \sum_{h=1}^{H} \left[RE(i,h) \times \frac{\phi_H(i,h)}{\phi_{H,avg}} \right] , \quad (35)$$

where the average scalar flux is

$$\phi_{H,avg} = \frac{1}{I \times H} \sum_{i=1}^{I} \sum_{h=1}^{H} \phi_H(i,h) , \quad (36)$$

$$err_{rms} = \sqrt{\frac{\sum_{i=1}^{I} \sum_{h=1}^{H} RE(i,h)^2}{I \times H}} , \quad (37)$$

and

$$err_{\max} = \max RE(i,h) \quad \text{for all } i \text{ and } h . \quad (38)$$

Results for assemblies 1 and 4 are given in Table I as they give a good breadth of the capabilities of the method. Assembly 4 is by far the most constraining assembly because of the high gadolinium loading. The reported computational time for the one group with expansion also includes the time needed to generate the cross-section moments.

As is seen in Table I, the DGM method gives an accurate flux solution while the computational time is much less than the fine-group calculation. The values of the average relative error, mean relative error, root mean square relative error, and maximum relative error of assembly 4 are larger than those of assembly 1 because of the strong heterogeneities of assembly 4 caused by the presence of gadolinium. The mean relative error is an average error in which the relative errors are weighted by the flux values. For assembly 4, the mean relative error is much smaller than the average relative error, which indicates that the larger errors occur in regions of very low flux (i.e., thermal groups in the Gd-rich regions).

The eigenvalues from the DGM method are equivalent to the ones that would be obtained from one-group

TABLE I

Assemblies 1 and 4 Calculation Results

	err_{avg} (%)	err_{mean} (%)	err_{rms} (%)	$err_{\max}$ (%)	Eigenvalue k	Computational Time (s)
Assembly 1 8-group	2.48E−4[a]	1.47E−4	3.46E−4	1.20E−3	1.240588	0.3
Assembly 1 1 group/expansion					1.240576	0.03
Assembly 4 8-group	1.45E−2	9.84E−4	5.23E−2	3.06E−1	0.323416	0.2
Assembly 4 1-group/expansion					0.323416	0.02

[a]Read as 2.48×10^{-4}.

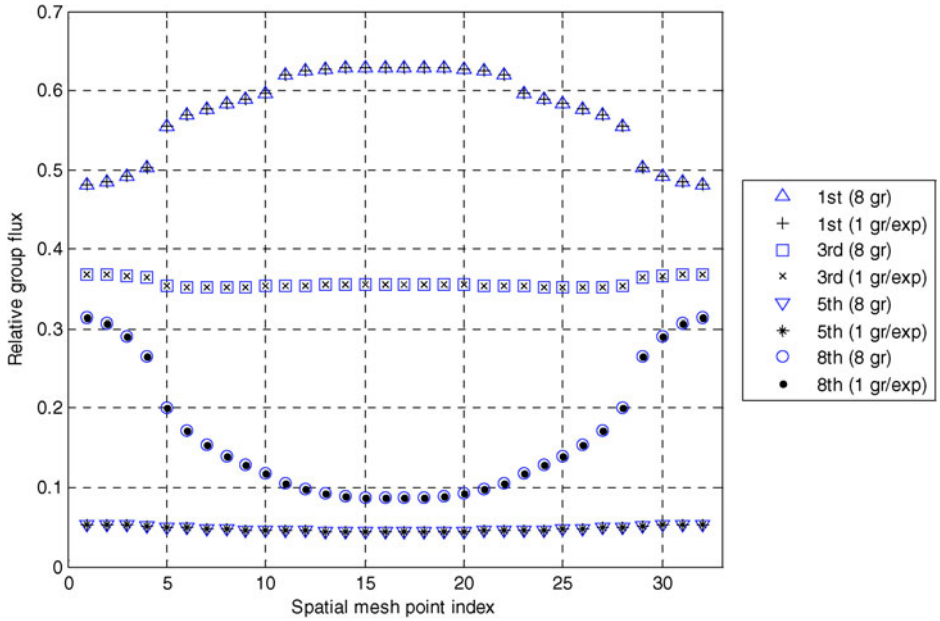

Fig. 4. Assembly 1 scalar flux comparison between 8-group and 1-group with 7-order expansion calculations.

calculations. Thus, the DGM method, at this point, only provides an accurate eight-group representation of the flux for much less effort than the reference calculation. Figures 4 and 5 plot the relative group flux in assemblies 1 and 4 as a function of spatial mesh point index for different groups. As Figs. 4 and 5 show, the DGM method can reproduce very accurately the fine-group solution.

IV.B. Whole-Core Tests

Now that the methodology has shown the ability to reproduce the reference flux solution, a tougher test is needed to illustrate the advantages of the DGM method for whole-core calculations. A comparison is made between 47 group reference solutions for the three cores of

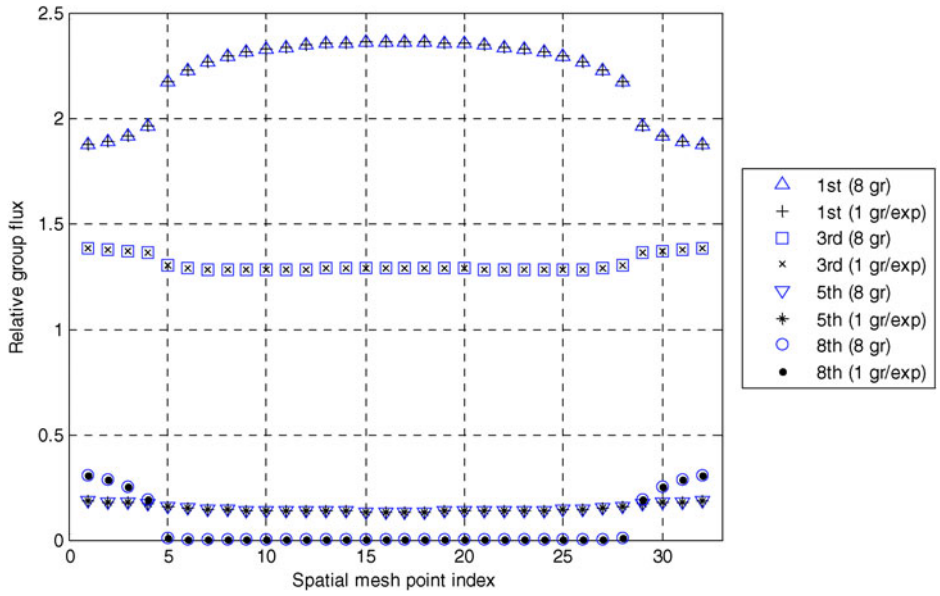

Fig. 5. Assembly 4 scalar flux comparison between 8-group and 1-group with 7-order expansion calculations.

Fig. 3 with a 2-group DGM calculation with respective expansion orders of 34 and 11. The 47 group cross sections were generated from the HELIOS lattice depletion code (Ref. 7 and HELIOS), in which the first 35 groups are in the fast region above the thermal cutoff of 0.625 eV while groups 36 to 47 cover the thermal energy range. Once again, an S_{16} angular approximation is applied, and the step difference method is used for the spatial sweep. The flux is converged to within 10^{-5}, and the eigenvalue is converged to within 10^{-6}. Vacuum boundary conditions are set on both sides.

In this calculation, the two-group cross sections with moments needed in the DGM method are not generated from the reference solution but from fine-group assembly calculations (such as would be done in current multilevel calculations). Table II lists the flux error measures, eigenvalue, and the computational time (including the calculation time needed for obtaining the cross-section moments) for cores 1 and 3. The results for core 2 were omitted from the discussion since they fall somewhere between the results of cores 1 and 3. From Table II, the computational time of the DGM method is very small compared to the fine-group calculation. Again, the eigenvalues from the DGM method are equivalent to the ones from the coarse-group calculations.

In core 1, the average relative error, mean relative error, and root mean square relative error are on the order of 1 to 4%, while they are about an order of magnitude larger in core 3, once again due to the strong heterogeneities introduced by the many instances of assembly 4 (with gadolinium). In core 3, the maximum relative error seen is 640%, which happens in the 47th group (most thermal) in which the flux is almost zero because of the presence of Gd. At this particular location of maximum flux error, the scalar flux from the fine-group calculation is 4.62×10^{-6}, and the value from the DGM method is -2.50×10^{-5}. Both of these values are very small by comparison to the flux in other locations in the core, and the unfolded flux also has an unphysical negative value, which can explain the large relative error. These results will be improved on in Sec. IV.C by the introduction of the source updating procedure.

The issue that was identified with the DGM method is that if a particular group flux at a particular spatial point is very small and near zero, i.e., the 47th group in the Fuel + Gd regions, it is possible that the DGM method will give a slightly negative flux at some spatial points. While this issue has been shown to happen in the results for core 3, it should be noted that in core 1, which does not contain gadolinium, and all single-assembly cases, no negative fluxes were observed from the DGM calculation. In single-assembly calculations, the cross-section moments were generated with the exact reference spectrum, while in the whole-core calculations, as done in the standard multilevel approach, the cross-section moments were generated from fine-group assembly calculations. Thus, the combination of inaccurate spectrum to generate cross sections and the strong heterogeneities of the core due to the presence of gadolinium led to the negative fluxes and large maximum relative errors as observed in core 3. The following update procedure, which takes advantage of the discrete nature of the DGM method, can eliminate this occurrence and improve the eigenvalue and flux errors.

IV.C. Eigenvalue and Flux Updates

In the previous results, the DGM method has been shown to provide accurate expanded fluxes, but it maintained the same coarse-group eigenvalue. At this point, integral quantities, i.e., the eigenvalue and reaction rates, are not improved and are identical to those obtained from the standard coarse-group calculation.

TABLE II

Cores 1 and 3 Calculation Results

	err_{avg} (%)	err_{mean} (%)	err_{rms} (%)	$err_{\max}$ (%)	Eigenvalue k	Computational Time (s)
Core 1 47-group	2.73	1.77	4.17	4.17E+1[a]	1.151877	161
Core 1 2-group/expansion					1.165302	2.3
Core 3 47-group	1.60E+1	9.02	3.10E+1	6.40E+2	0.722289	153
Core 3 2-group/expansion					0.791960	2.4

[a]Read as 4.17×10^{1}.

Since the expanded flux shape is very accurate and comparable to the fine-group reference flux shape and is much more accurate than the coarse-group flux shape, which is piecewise flat within each coarse group, the eigenvalue can be updated by simple neutron balance, using the obtained expanded flux and the reference fine-group cross-section data:

$$k_{update} = \frac{\text{Production}}{\text{Absorption} + \text{Leakage}} = \frac{\sum_{i=1}^{I}\sum_{h=1}^{H} \upsilon\sigma_f(i,h)\phi_{G/\exp}(i,h)\Delta_i}{\sum_{i=1}^{I}\sum_{h=1}^{H} \sigma_a(i,h)\phi_{G/\exp}(i,h)\Delta_i + \sum_{m=1}^{M}\sum_{g=1}^{G} \mu_m w_m \psi_{G,b}(m,g)} \quad , \tag{39}$$

where the fission and absorption terms are calculated using the unfolded expansion scalar flux and fine-group cross sections, and the leakage term is calculated using the coarse-group (leading-order) angular boundary flux $\psi_{G,b}$, and where Δ_i is the spatial mesh width; μ_m and w_m are abscissas and weights of Gauss-Legendre quadrature for $m = 1, \ldots, M$; and h, g, and i are fine-group, coarse-group, and spatial mesh point indices.

After updating the eigenvalue, the angular flux is updated to eliminate possible negative angular fluxes. On the right side of Eq. (10), for each fine group h, the fission and scattering fixed source can be calculated using the updated eigenvalue, the unfolded expansion flux, and the fine-group cross sections:

$$Q(\vec{r},\vec{\Omega},K) = \sum_{g'=1}^{G}\sum_{l=0}^{\infty}\sum_{m=-l}^{l} \frac{Y_{lm}^{*}(\vec{\Omega})}{4\pi} \sum_{L=0}^{M-1} \sigma_{sl}(\vec{r}, L \rightarrow K) \times \phi_{lm}(\vec{r},L) + \frac{\chi(\vec{r},K)}{4\pi k} \times \sum_{g'=1}^{G}\sum_{L=0}^{M-1} \nu\sigma_f(\vec{r},L)\phi(\vec{r},L) \quad , \tag{40}$$

where $k = k_{update}$, and $\phi_{lm}(\vec{r},L)$ and $\phi(\vec{r},L)$ are from the DGM calculation. With this new more accurate driving source, the left side of Eq. (10) can be reevaluated as a fixed-source problem:

$$\vec{\Omega}\cdot\nabla\psi_{update}(\vec{r},\vec{\Omega},K) + \sigma_t(\vec{r},K)\psi_{update}(\vec{r},\vec{\Omega},K) = Q(\vec{r},\vec{\Omega},K) \quad . \tag{41}$$

Each such flux update is very quick since it is a fixed-source problem and no source iteration is required. In the reported results with negative angular fluxes, it was observed that a single flux update was enough to eliminate all negative angular fluxes, and the errors are also improved when compared to the fine-group reference solution.

Table III lists the results obtained after the updates of the eigenvalue k and the flux. The computational time of the updates is very small compared to that of the coarse-group calculation. By comparing Tables II and III, the eigenvalue and the flux errors improve slightly.

For core 1, the average relative error, mean relative error, and root mean square error are on the order of 1 to 3%, which is marginally better than before the update. The maximum error, however, is substantially reduced

TABLE III

Cores 1 and 3 Calculation Results After the Updates of Eigenvalue and Flux

	err_{avg} (%)	err_{mean} (%)	err_{rms} (%)	$err_{\max}$ (%)	Eigenvalue k	Computational Time (s)
Core 1 47-group	2.39	1.60	3.20	1.41E+1[a]	—	—
Core 1 2-group/expansion + update					1.163845	0.3
Core 3 47-group	1.28E+1	8.43	1.51E+1	3.18E+1	—	—
Core 3 2-group/expansion + update					0.780053	0.3

[a]Read as 1.41×10^6.

from 41.7 to 14.1%. For core 3, the average relative error, mean relative error, and root mean square error are also reduced quite a bit. Of note the root mean square error dropped from 31.0 to 15.1%. The maximum relative error is also reduced considerably from 640 to 31.8% before and after the update. These errors arise from the inaccurate spectrum used to generate the cross-section moments of each assembly, but for very little added computational cost, they can provide improved results over a coarse-group calculation.

By adding the computational times of the expansion calculation and the times of the eigenvalue and flux updates in Tables II and III, the total times required to perform the DGM calculation plus the updates are 2.6 s for core 1 and 2.7 s for core 3. In comparison, the computational times of the fine-group calculations are 161 s for core 1 and 153 s for core 3. Thus, the computational time of the DGM method plus the updates is $<2\%$ of that of the standard fine-group reference calculation.

Figures 6 through 9 plot the relative group fluxes in cores 1 and 3 as a function of spatial mesh point index for different energy groups. Note that the expanded fluxes are the values after the update process and thus have no negative values. In Figs. 6 through 9, only half the core is represented (symmetric core), and one in every three spatial points is plotted to avoid unnecessary cluttering. In the fast energy region, the two groups with the highest total reaction rates (groups 9 and 11 for both cores) and two groups in the resonance region corresponding to the two important ^{238}U resonances, i.e., 6.67 eV (group 19) and 20.8 eV (group 15) for both cores are plotted. In the thermal energy region, the group with the highest fission rate, i.e., group 43 for both cores, and the group with the highest group scalar flux, i.e., group 39 for both cores, are plotted. As Figs. 6 through 9 show, the DGM method can reproduce very accurately the fine-group solution. Even in core 3, with the presence of gadolinium, the flux from the DGM calculation matches the fine-group reference calculation very accurately. It can be observed that the fluxes in the thermal groups (plotted in Fig. 9) are all very small in the Fuel+Gd regions.

IV.D. Further Updates

Up to this point the integral quantities have been improved through the above update procedures. Since more accurate flux values are obtained, further improvement is possible by repeated application of Eqs. (39), (40), and (41) in which the scalar flux and boundary angular flux values are from the previous update calculations. Computational cost of such updates is the same as given in Table III. Note that in Eq. (39), for the following eigenvalue updates, boundary angular flux has a fine-group structure. Normalization to the fission source needs to be performed before each new flux update calculation. A successive update procedure thus becomes a fine-group solution in which the DGM solution was used as an initial guess. The DGM method could thus also be pursued as an acceleration method for the fine-group calculation.

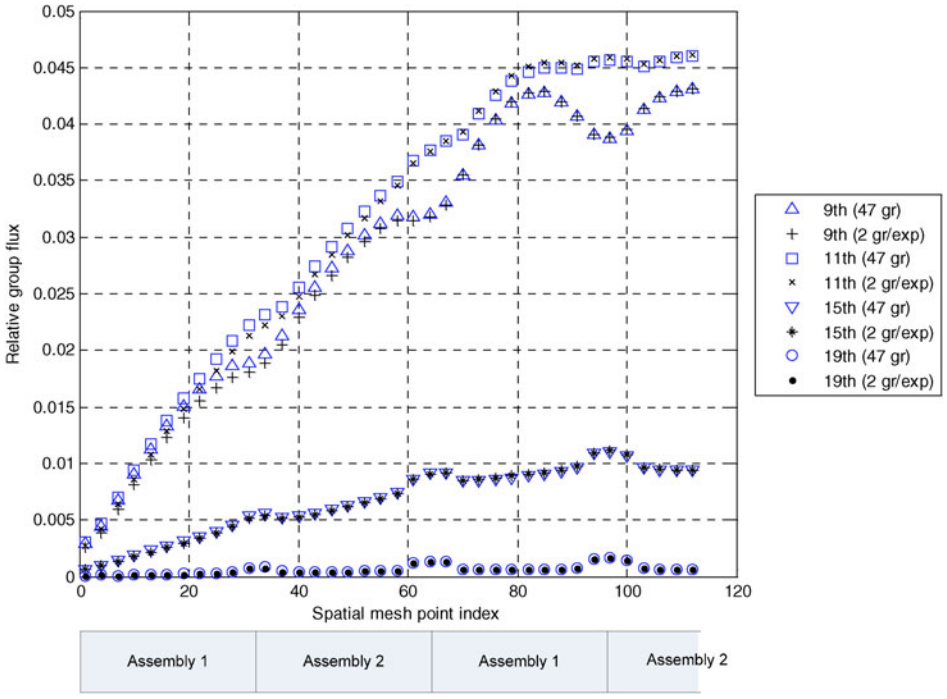

Fig. 6. Core 1 scalar flux comparison between 47-group and 2-group-with-expansion calculations (fast groups).

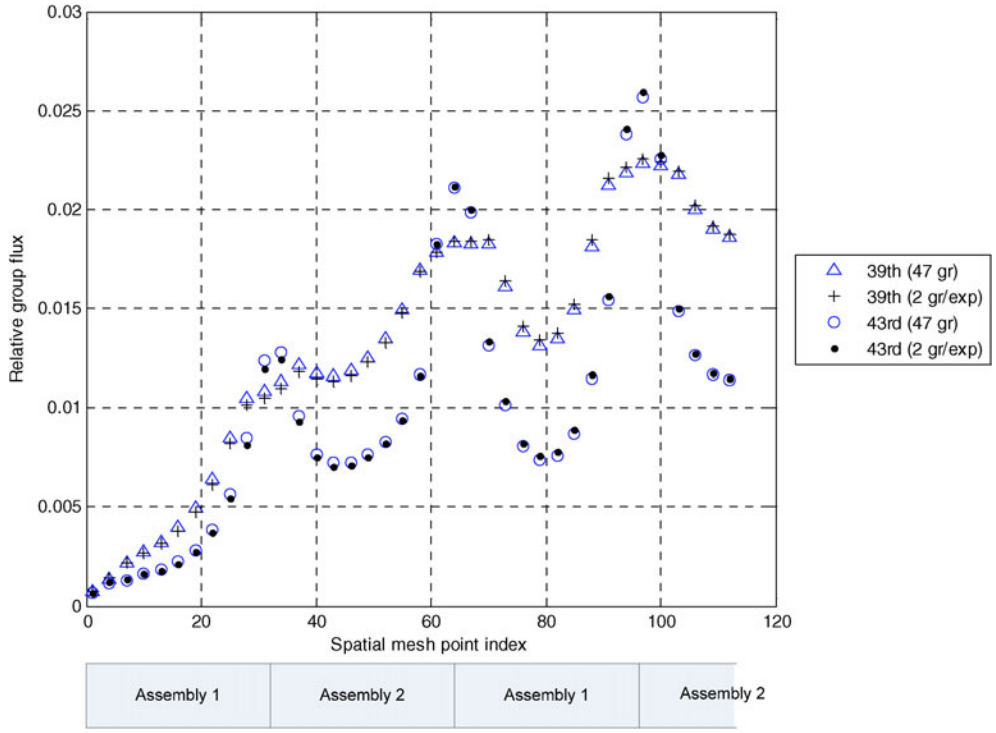

Fig. 7. Core 1 scalar flux comparison between 47-group and 2-group-with-expansion calculations (thermal groups).

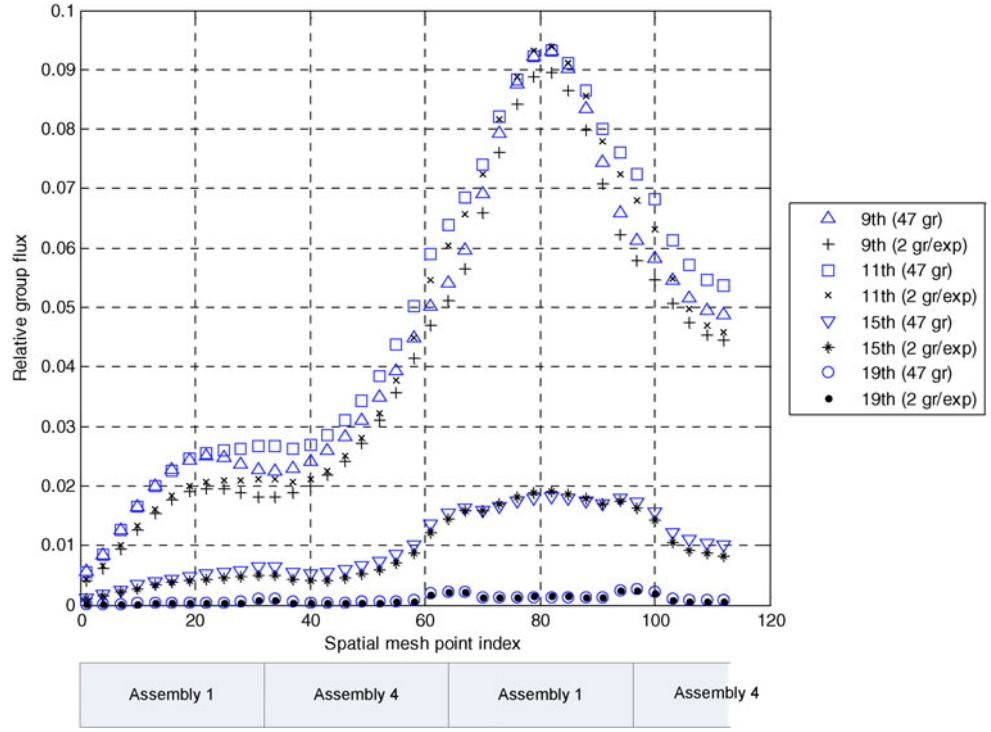

Fig. 8. Core 3 scalar flux comparison between 47-group and 2-group-with-expansion calculations (fast groups).

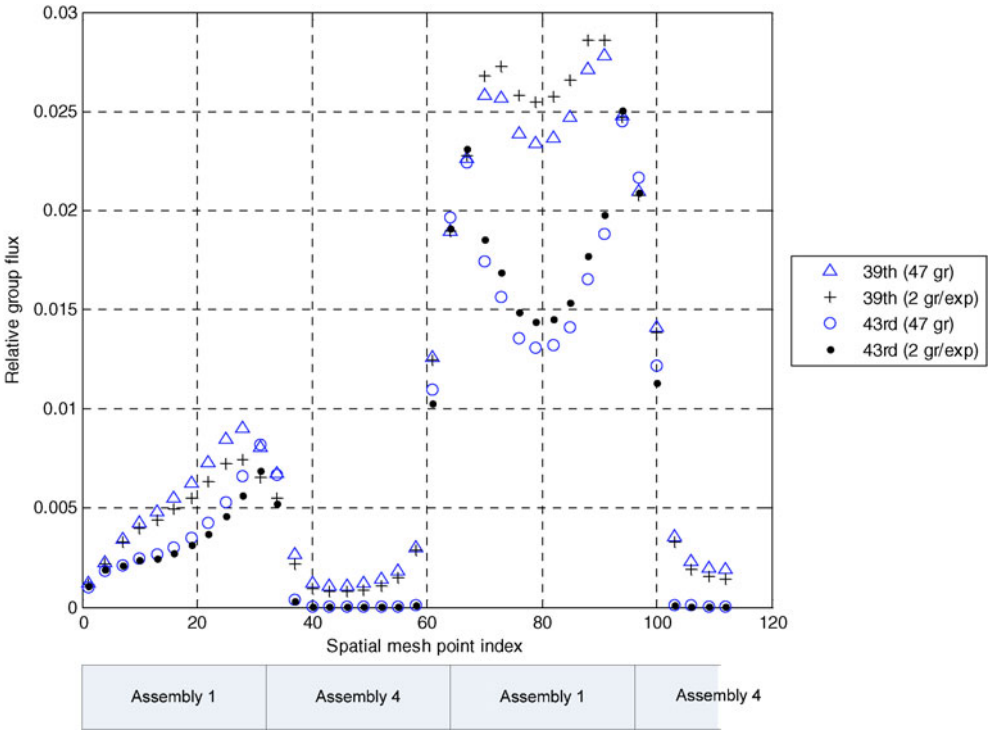

Fig. 9. Core 3 scalar flux comparison between 47-group and 2-group-with-expansion calculations (thermal groups).

V. CONCLUSIONS AND FUTURE WORK

In this study, the DGM method has been developed by expanding the energy dependence of the angular flux to a set of flux moments. Fine-group assembly solution is used as the weighting function for the generation of the discrete cross-section moments that are used to solve the flux in the core for each expansion moment. The obtained flux moments are unfolded to construct a whole-core energy spectrum. The obtained spectrum is an accurate estimate to the fine-group solution.

Based on the properties of the DLOP expansion basis, the zeroth-order equation is decoupled from the higher-order equations. This decoupling leads to reaction rates and eigenvalue that at first glance are no better than the equivalent coarse-group calculations but provide an accurate fine-group spectrum with little computational cost. An additional advantage of the discrete expansion is the possibility of updating the integral parameters by using the expanded flux with the fine-group data, thus providing more accurate eigenvalue and reaction rates. Furthermore, this additional step also eliminates all unphysical negative flux values.

The new method has been tested through a series of 1-D BWR cores and assemblies using a 1-D discrete ordinates code. For the single-assembly calculations in which the exact reference spectrum was used to generate the cross-section moments, the DGM method reproduced accurately the fine-group spectrum. For the whole-core 1-D calculations in which fine-group assembly spectrum was used to generate the cross-section moments, results have shown that the DGM method can provide a reasonable estimate to the fine-group spectrum in the whole core. The average relative error, mean relative error, and root mean square error are on the order of a few percent in core 1, while they are on the order of 10% in core 3, which is the most heterogeneous case studied. The computational cost of the DGM method including a source update is $<2\%$ of that from the standard fine-group reference calculation. More updates can be performed to further decrease the errors, but these would essentially amount to performing the fine-group calculation.

Since the DGM method can provide a very accurate estimate to the fine-group spectrum, it brings many possibilities such as using this approach as an acceleration scheme for fine-group solutions or the introduction of an energy recondensation process that could potentially eliminate the need for multilevel calculations. These possibilities are currently being investigated as well as an extension to more realistic 3-D geometries.

REFERENCES

1. E. E. LEWIS and W. F. MILLER, Jr., *Computational Methods of Neutron Transport*, American Nuclear Society, La Grange Park, Illinois (1993).

2. M. L. WILLIAMS, M. ASGARI, and D. F. HOLLENBACH, "CENTRM: A One-Dimensional Neutron Transport Code for Computing Pointwise Energy Spectra," ORNL/TM-2005/39, Version 5.1, Vol. II, Book 4, Sect. F18, Oak Ridge National Laboratory (2006).

3. M. L. ZERKLE, I. K. ABU-SHUMAYS, M. W. OTT, and J. P. WINWOOD, "Theory and Application of the RAZOR Two-Dimensional Continuous Energy Lattice Physics Code," *Proc. Joint Int. Conf. Mathematical Methods and Supercomputing for Nuclear Applications*, Saratoga Springs, New York, October 5–9, 1997, Vol. 1, p. 417, American Nuclear Society (1997).

4. I. K. ATTIEH and R. E. PEVEY, "An Adaptive General Multigroup Method," *Proc. 27th Annual CNS-CNA Student Conference*, Toronto, Ontario, Canada, June 2–5, 2002.

5. D. F. CARBON, "A Comparison of the Straight-Mean, Harmonic-Mean, and Multiple-Picket Approximations for the Line Opacities in Cool Model Atmospheres," *Astrophys. J.*, **187**, 135 (1974).

6. B. FORGET and F. RAHNEMA, "A Spectral Unfolding Method," *Trans. Am. Nucl. Soc*., **96**, 669 (2007).

7. F. RAHNEMA, S. DOUGLASS, and B. FORGET, "Generalized Energy Condensation Theory," *Nucl. Sci. Eng*., **160**, 41 (2008).

8. C. P. NEUMAN and D. I. SCHONBACH, "Discrete (Legendre) Orthogonal Polynomials—A Survey," *Int. J. Numer. Methods Eng*., **8**, 743 (1974).